High Voltage

Research Article

IET Journals
The Institution of Engineering and Technology

Investigation on thermally aged natural ester oil for real-time monitoring and analysis of transformer insulation

eISSN 2397-7264
Received on 18th July 2019
Revised 17th October 2019
Accepted on 1st November 2019
E-First on 6th February 2020
doi: 10.1049/hve.2019.0178
www.ietdl.org

Arputhasamy Joseph Amalanathan[1], Ramanujam Sarathi[1] ✉, Swayam Prakash[2], Ashok Kumar Mishra[2], Ribhu Gautam[3], Ravikrishnan Vinu[3]

[1]*Department of Electrical Engineering, Indian Institute of Technology Madras, Chennai 600036, India*
[2]*Department of Chemistry, Indian Institute of Technology Madras, Chennai 600036, India*
[3]*Department of Chemical Engineering, Indian Institute of Technology Madras, Chennai 600036, India*
✉ *E-mail: rsarathi@iitm.ac.in*

Abstract: Thermal aging of natural ester oil shows drastic reduction in partial discharge inception voltage (PDIV) and a significant variation is observed only above a certain aging time, under AC, DC, high frequency AC voltages and with harmonic voltages with different total harmonic distortion. Weibull distribution studies on PDIV measurements indicate a reduction in scale parameter (α) with increase in thermal aging temperature. A characteristic reduction in breakdown voltage was observed with the thermally aged ester oil, under AC, DC and standard lightning impulse voltage. The breakdown voltage variation with aged ester oil follows normal distribution. Ultraviolet (UV) analysis of ester oil thermally aged at 160°C has revealed a regular shift of the derived absorbance parameter to longer wavelengths. The interfacial tension and turbidity exhibits an inverse relationship with the thermally aged ester oil. Gas chromatography/mass spectrometric analysis of the thermally aged ester oil predicted the formation of more carboxylic acids and ketones with aging duration. The steady-state fluorescence on thermally aged ester oil exhibits a shift in its emission profile, which is in tandem with the UV absorption spectroscopic analysis. Fluorescence analysis can be adopted as a real-time monitoring tool in transformers, to understand the condition of liquid insulation. The viscosity dependence on the wavelength of derivative absorption maxima follows a direct relationship with the thermally aged natural ester oil.

1 Introduction

Transformer forms the heart of the power system network. Conventionally, in oil-filled transformers, mineral oil is used as an insulant and as a coolant. In service, the liquid insulant is subjected to multiple stresses caused by electrical, thermal and chemical reactions such as oxidation, the formation of acids and hydrolysis that lead to a characteristic change in fundamental properties of the oil causing a reduction in the service life of the transformer [1]. Recently, ester-based oils are gaining importance as promising insulants to use in distribution transformers. The ester oil provides a higher benefit-to-cost ratio, draws the moisture out from cellulose with a higher AC breakdown strength and is biodegradable [2, 3]. Mehta *et al.* have clearly indicated the need for understanding dielectric, thermal and physical properties and issues with the ester-based oil before its use as insulant in transformers [4].

In transformers, the oil temperature can rise to about 160°C due to hot spot formation, which can cause severe damage to solid and liquid insulants [5, 6]. When the insulation is overstressed by high temperature, chemical bonds in the oil and cellulosic pressboard may break, resulting in the formation of degradation products. One of the major causes for the failure of transformer insulation is the occurrence of corona due to the protrusion from the winding conductor. Considerable works were carried out to understand the breakdown characteristics of ester oil under AC voltages [7]. Now with the increased use of power electronic devices, it has become essential to know the partial discharge (PD) activity in ester oil, under high frequencies and harmonic AC voltages with different total harmonic distortion (THD)'s [8]. Identification of such incipient discharges is a real challenge and various techniques are adopted to identify these discharges including phase-resolved PD (PRPD) analysis, acoustic emission technique, dissolved gas analysis, chemical analysis and RF technique [9].

It is now well established that the injected current pulse due to PDs in transformer oil has a rise time of a few nanoseconds, which excites electromagnetic signals in the ultra high frequency (UHF) range, i.e. 300–3000 MHz [10]. The characteristics of UHF signal formed due to PD activity with ester oil/thermally aged ester oil need to be understood. Huang *et al.* [11] studied the PD activity in ester oil and have indicated that PD activity is high in the positive half cycle and less in the negative half cycle. Florkowski *et al.* [12] have studied PD activity in transformer insulation system under harmonic AC voltages and have indicated that the rate of change of voltage has a high impact on the discharge activity. It is essential to understand the characteristic variation in PRPD pattern with thermally aged ester oil. Rozga [13] indicated that the breakdown strengths of ester oil and mineral oil under lightning impulse voltage are nearly the same. It is essential to understand the impact of thermal aging of ester oil and its breakdown characteristics under standard lightning impulse voltage.

It is also necessary to study the characteristic changes in the composition of organic compounds in thermally aged ester oil, as the degradation compounds can destabilise the oil. Marin-Serrano *et al.* [14] utilised ultraviolet (UV)–visible spectrophotometry and infrared spectroscopy to understand the characteristic variation in properties of mineral oil due to thermal aging. Bessant *et al.* [15] indicated that the fluorescence monitoring of transformer oil could be used as a condition monitoring tool for transformers. Synchronous fluorescence spectroscopy (SFS) and excitation–emission matrix fluorescence (EEMF) techniques were used to monitor the aging related fluorescence spectral changes of mineral oil. Thermally stressed edible oils were characterised using SFS, EEMF spectra and PARAFAC modelling [16]. In recent times, time-resolved fluorescence spectroscopy using time-correlated single-photon counting technique has been gaining importance. This methodology allows to characteristic variation during the lifetime of fluorescence and can be adopted for condition monitoring. In general, the adoption of such techniques enable one to understand the impact of thermal aging of ester oil.

Having known all this, methodical experimental studies were carried out to understand the fundamental properties of thermally

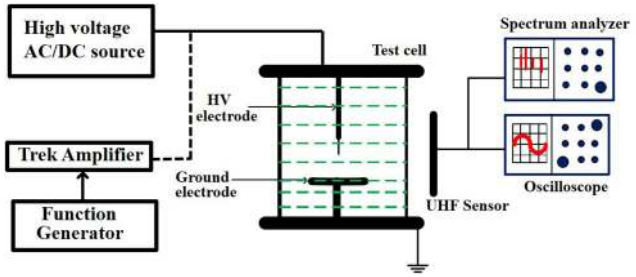

Fig. 1 *Experimental setup for partial discharge and breakdown studies*

aged ester oil, through following important studies (i) variation in PD inception voltage (PDIV) with thermally aged ester oil under AC, high-frequency AC, DC voltage and harmonic AC voltage with different THD's, (ii) statistical analysis on breakdown strength of thermally aged ester oil under AC and DC voltages, (iii) analysis of UHF signal generated due to PD activity under AC and DC voltages, (iv) analysis of thermally aged ester oil by UV, fluorescent analysis and by pyrolytic GC/MS studies and (v) analysis of viscosity and turbidity of thermally aged ester oil.

2 Experimental studies

The experimental set-up used for generating the PD and for breakdown studies is shown in Fig. 1. The test arrangement includes a high voltage source, test electrode and UHF sensor along with digital storage oscilloscope (DSO).

2.1 High-voltage source

A 100 kV, 5 kVA, 50 Hz transformer was used to generate the required AC voltage and a voltage doubler circuit was used to generate the DC voltage. The capacitance and resistance divider was used to measure the applied AC and DC voltages, respectively. The high-frequency AC voltage and harmonic AC voltage with different THD's were generated by use of high voltage Trek amplifier (Model 20/20C) with desired input waveshape using a function generator. The voltage applied for the test was increased at a constant rate of 300 V/s. The standard lightning impulse voltage (1.2/50 μs) was generated with a single-stage impulse generator. Capacitance divider was used for its measurement.

2.2 Test cell and breakdown studies

Needle-plane electrode configuration was used for PD and breakdown studies. The distance between the needle and the bottom ground electrode was maintained at 5 mm. The stainless steel needle with its tip radius of 50 ± 3 μm and the ground electrode with 5 cm in diameter was used for the study. For every ten breakdowns, the needle electrode was replaced, for experimental studies, to avoid variation in breakdown voltage due to needle electrode tip radius variation. After every breakdown, the gap between the needle electrode and the ground is free from any carbon track or bubbles formed due to previous breakdown. New oil is used in the study, after every 25 breakdowns.

2.3 UHF sensor

Non-directional broadband UHF sensor was used for identifying the PD activity generated UHF signals [17]. The sensor was kept at a distance of 20 cm away from the test cell. The output of the sensor was connected to the DSO that has a bandwidth of 3.5 GHz operated at 40 GSa/s with an input impedance of 50 Ω/ spectrum analyser.

2.4 Thermal aging

Natural ester oil (MIDEL 1215) was used for thermal aging studies. The pressboard material with a thickness of 1.5 mm was wrapped with the copper sheet and immersed into a beaker with 650 mL of natural ester oil. The weights of the pressboard, copper sheet, and oil were taken in the ratio of 1:1:10. The thermal aging was carried out at 90, 140 and 160°C in nitrogen gas ambiance as per IEC 62332-2 standard [18]. The oil samples were taken out at every 100 h from the reaction mixture, for further analysis.

2.5 Physico-chemical studies

Electronic absorption spectra were measured with a Shimadzu V-2500 A1 UV–visible spectrophotometer with a scan rate of 1 nm. Fluorescence measurements were performed with a Horiba aqualog spectrofluorometer with a xenon lamp of 150 W. A triangular cuvette was used in order to obtain both front and back-face fluorescence with minimum scattering. EEMF spectra were measured in the excitation wavelength range of 240–700 nm at an interval of 10 nm. The emission wavelength range was set at 240–800 nm with an interval of 1.1 nm. All fluorescence measurements of the oil samples were taken at a regular interval of 100 h, in order to detect the marginal variation in the degradation mechanism of ester oils until the total aging period of 500 h.

Viscosity measurements were performed in a modular compact rheometer (MCR 102, Anton Paar) with a CP 40 Cone and Plate measuring system. Turbidity measurements were carried out using Nephlo-Turbidity metre. Dynamic contact angle tensiometer with a Wilhelmy plate made up of platinum and iridium was used for measuring interfacial tension (IFT). GC/MS spectrometer (Shimadzu QP2010 Plus) was used to estimate the organic composition of fresh and thermally aged ester oil. At the first stage, the ester oil was diluted to 1000 ppm with chloroform and 1 μL was injected to the UA-5 capillary column (5% dimethylpolysiloxane, 30 m × 0.25 mm i.d. × 0.25 μm film thickness). The GC oven was initially maintained at 40°C for 1 min and increased to the required temperature of 280°C, at the heating rate of 10°C min^{-1} and finally maintained at this temperature for 10 min. Ultra high pure helium (99.9995%) was used as the carrier gas at the column flow rate of 1 mL min^{-1} with a split in ratio of 14.3:1. The injector, interface and ion source temperatures were 300, 300 and 250°C. The pyrolysates were scanned in the m/z range of 50–500 Da (m/z) and the products were identified using NIST library of the mass spectra of organic compounds. The pyrolysates composition obtained by using relative peak area %. The experiments carried out for three times and the product yields, its standard deviation was within 5%.

3 Results and discussion

3.1 Variation in PDIV of thermally aged ester oil

Fig. 2 shows the variation in PDIV of thermally aged ester oil under different voltage profiles. In the present study, the PDIV was measured based on the first pulse being captured by the oscilloscope from the UHF sensor output. It is observed that, under AC and DC voltages, the PDIV decreases with both aging temperature and aging time. This variation is significant with virgin ester oils and with thermally aged ester oil. It is also observed that the PDIV is high under negative DC followed with positive DC and AC voltages.

The PD inception and its propagation get altered with the local condition including the radius of curvature of the top needle electrode, moisture content and contaminated particles present in the oil etc. [19]. Fig. 2 shows no major change in the PDIV under AC voltage upto 100 h and a marginal reduction was observed after 300 h of aging time. Also, the PDIV was less affected at lower aging temperature (90°C). When the aging temperature is high, the PDIV gets reduced and the standard deviation in its measured value was lower. Azcarraga *et al.* [20] have shown that the injected charges in the negative half cycle have a high impact on the inception of discharges. He has clearly indicated that local electric field has high impact on PD inception. The ionisation of the liquid at the needle tip under positive polarity produces an aiding electric field that initiates discharges at lower voltage as compared to negative polarity.

Xiang *et al.* [21] have studied the inception and breakdown characteristics of insulating liquids under DC stress. They have indicated that intensity of light and number of pulses that have occurred on occurrence of discharges is high under positive

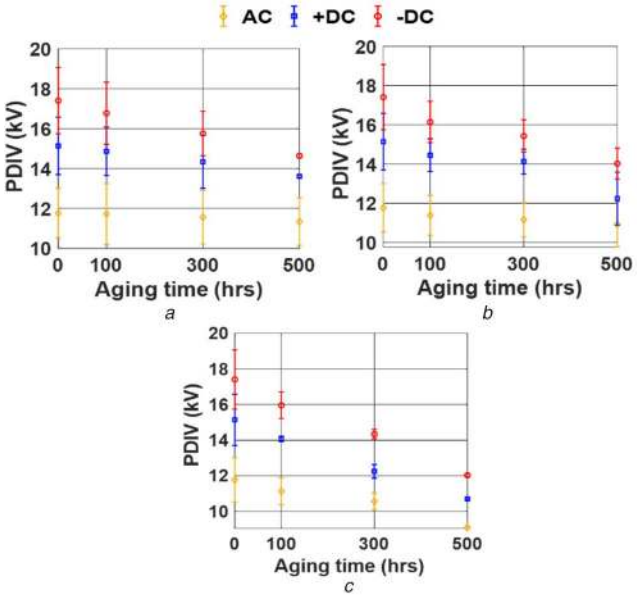

Fig. 2 *Variation in the PDIV of ester oil aged at different temperatures under different voltage profiles*
(a) 90°C, ***(b)*** 140°C, ***(c)*** 160°C

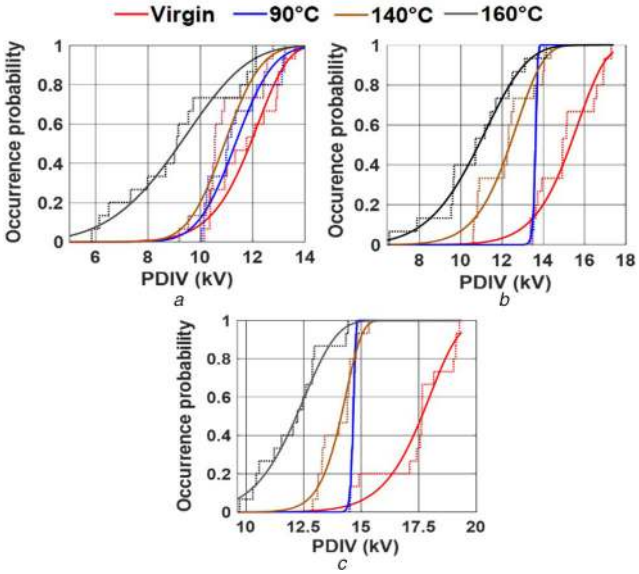

Fig. 3 *Weibull distribution of PDIV for virgin and thermally aged ester oil under different voltage profiles*
(a) AC voltage, ***(b)*** + DC voltage, ***(c)*** −DC voltage

polarity. Under negative DC voltage incepted discharges, they have indicated that intensity of light measured was much lower than that occurred under positive discharges. In addition, the number of pulses formed are discrete and its duration lies around 100 ns. This clearly indicates that the severity of discharges to be high under positive DC voltage. The PDIV was fitted with a two-parameter Weibull distribution as per the IEC 62539 standard [22] for statistical analysis [23] is shown in Fig. 3. The effect of scale parameter (α) with tip radius due to PD activity has been found to increase [20]. The scale parameter (α) measured with PDIV of thermally aged oil, for different voltage profile under different aging temperature was calculated (from Fig. 3) based on 63.2% probability percentile with a 95% confidence intervals, and is shown in Fig. 4. It is observed that the scale parameter decreases with increase in aging temperature.

Table 1 shows the variation in PDIV of ester oil under high-frequency AC voltage. It is evident that the increase in frequency leads to a reduction in PDIV. It is also observed that at a particular harmonic voltage, the influence of THD on PDIV is minimum (Table 2). The values in Table 2 is an average of 20 readings. The standard deviations, in this case, was <0.05 kV. Hence, the error values were not included in Table 1.

The typical UHF signal acquired during PD activity with thermally aged natural ester oil is shown in Fig. 5*a*. During the process of PD activity, around 50 sequences of signal were taken and its average FFT waveform has been indicated in Fig. 5*b*. Also, these sequences were repeated for multiple times and it was found that dominant frequency of all the signal lies around 1 GHz and an increase in the energy content of signal was also observed.

Fig. 6 shows the PRPD analysis of thermally aged ester oil at different temperatures under harmonic AC voltages with different THDs. It has been found that inception occurs at different voltages for different aged samples. Hence, in order to compare the different samples from PRPD analysis, the voltage was maintained at 20% above the PDIV and the PRPD signal was measured. PRPD analysis was carried out by connecting UHF sensor output to the spectrum analyser. The spectrum analyser was operated in zero span mode with central frequency same as the dominant frequency of 1 GHz generated due to PD activity (Fig. 5*b*). The function generator output used for applying voltage across the test cell by using Trek amplifier is synchronised with the spectrum analyser, to correlate the discharge activity with the phase of occurrence of the applied AC voltage. It is observed that PD activity in the negative half cycle is less compared to the positive half cycle, under

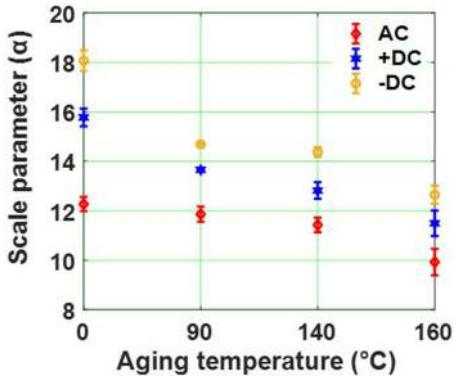

Fig. 4 *Statistical Weibull scale parameter for different aging temperature under different voltage profiles*

Table 1 Variation in the PDIV of thermally aged ester oil under high-frequency AC harmonics

Sample	PDIV, kV											
	2*f*			3*f*			5*f*			7*f*		
Virgin	11.71			11.65			11.43			11.24		
Aging temp/ aging time	100 h-aged sample	300 h-aged sample	500 h-aged sample	100 h-aged sample	300 h-aged sample	500 h-aged sample	100 h-aged sample	300 h-aged sample	500 h-aged sample	100 h-aged sample	300 h-aged sample	500 h-aged sample
90°C	11.67	11.58	11.39	11.58	11.43	11.26	11.48	11.27	10.95	11.17	11.04	10.76
140°C	11.53	11.31	10.86	11.42	11.12	10.69	11.26	10.96	10.43	10.96	10.71	10.35
160°C	11.51	11.02	10.52	11.22	10.86	10.24	11.12	10.47	10.21	10.45	10.12	9.43

Table 2 Variation in the PDIV of thermally aged ester oil under high-frequency AC harmonics with different THDs

Sample	PDIV, kV											
	f + 3*f* (4% THD)			*f* + 7*f* (4% THD)			*f* + 3*f* (40% THD)			*f* + 7*f* (40% THD)		
Virgin	11.54			11.12			10.56			10.35		
Aging temp/ aging time	100 h-aged sample	300 h-aged sample	500 h-aged sample	100 h-aged sample	300 h-aged sample	500 h-aged sample	100 h-aged sample	300 h-aged sample	500 h-aged sample	100 h-aged sample	300 h-aged sample	500 h-aged sample
90°C	11.48	11.25	11.16	11.08	10.78	10.61	10.32	10.26	10.01	10.19	9.94	9.76
140°C	11.12	10.75	10.43	10.83	10.32	10.07	10.13	9.67	9.54	9.87	9.54	9.13
160°C	10.57	10.11	9.75	10.05	9.78	9.22	9.96	9.34	9.02	9.23	8.75	8.23

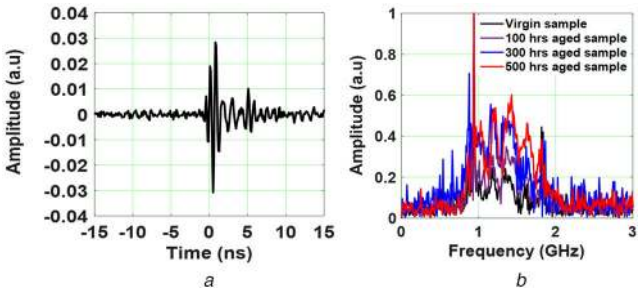

Fig. 5 *Typical UHF signal generated due to*
(a) PD activity, ***(b)*** FFT analysis with thermally aged ester oil

harmonic AC voltage. Under AC voltage, the discharge occurred in the range of 60° to 120° phase angle in the positive half cycle and in the range of 220°–270° phase angle in the negative half cycle. This clearly indicates that the spread in the phase of occurrence is less under negative AC voltage. Under harmonic AC voltage, the PD activity is more pronounced when rate of the rise in voltage is high.

3.2 Variation of breakdown voltage on the thermal aging of ester oil

Fig. 7 shows the variation in the breakdown strength of thermally aged ester oil under standard lightning impulse voltage, with needle-plane configuration. The breakdown voltage of the sample was taken based on average of 25 breakdown voltage measurements. It has been observed that negative lightning impulse leads to higher breakdown voltage compared to positive lightning impulse voltage. Dang *et al.* [24] concluded that irrespective of the type of liquid, the stopping length of negative polarity is higher than the positive polarity. The ester oil aged at 90°C did not show any major variation in breakdown voltage with the aging time and also the standard deviation about the mean was very less compared to virgin ester oil. The impact of negative lightning on the thermally aged ester oil was very less compared to positive lightning and a drastic reduction was observed only at higher aging temperatures (140 and 160°C). Li *et al.* [25] indicated that acid contents formed as by-product due to thermal aging can have high

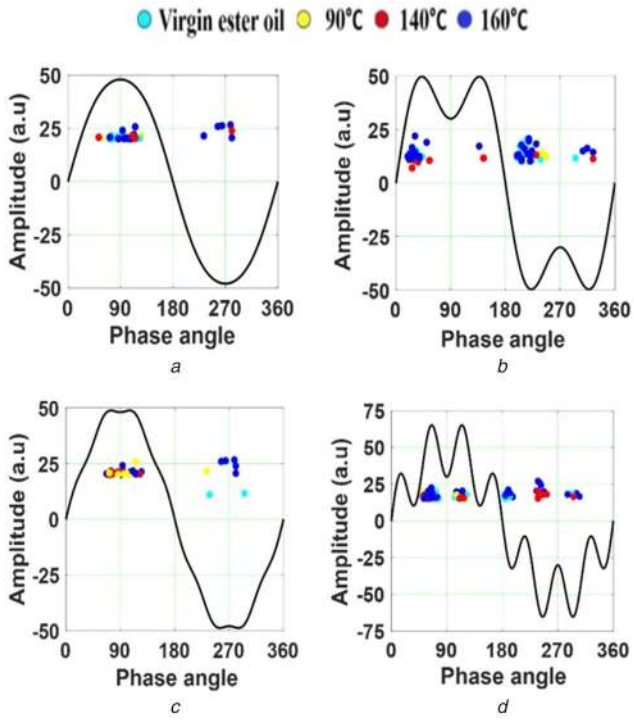

Fig. 6 *PRPD of thermally aged ester oils at different temperatures for 500 h aging duration*
(a) *f* + 3*f*(4%THD), ***(b)*** *f* + 3*f*(40%THD), ***(c)*** *f* + 7*f*(4%THD), ***(d)*** *f* + 7*f*(40%THD)

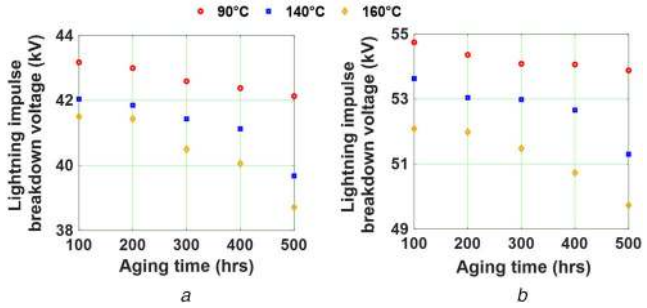

Fig. 7 *Analysis of impulse breakdown voltages of ester oil aged at different temperatures*
(a) Positive impulse, ***(b)*** Negative impulse

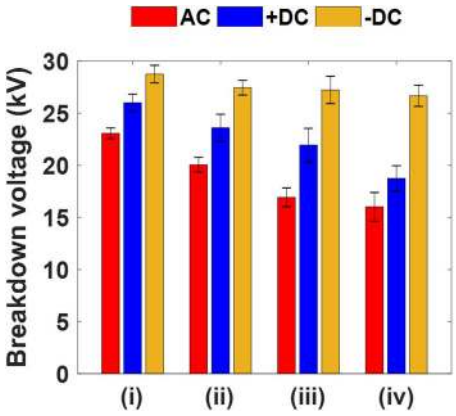

Fig. 8 *Variation in the breakdown voltage of thermally aged ester oil for 500 h aging duration (i) virgin ester oil, (ii) 90°C, (iii) 140°C and (iv) 160°*

impact on reduction in breakdown voltage, especially, under negative polarity than under positive polarity.

The variation in the breakdown voltage under AC and DC voltages are shown in Fig. 8 along with their standard deviation. It is observed that the breakdown strength of the electrode gap is high under negative DC voltage compared to positive DC and AC voltages. In case of the negative electrode, the streamers developed are highly branched and its propagation rate gets limited due to the lower diffusion of charge carriers which could have caused the reduction in the breakdown voltage to be more abrupt in both AC voltage and positive DC voltage compared to negative DC voltage.

The statistical analysis on the breakdown voltages of thermally aged ester oil was carried out using Shapiro–Wilk test in order to design and manage the power apparatus. The significance level of hypothesis was chosen as 95% to verify the data for normal distribution. The *p*-value is the probability of detecting the likelihood of hypothesis and it is also used to rank the distributions. If the *p*-value is higher than the significance level ($\alpha = 0.05$), then the null hypothesis is accepted. The *W* Statistic used for Shapiro–Wilk test is given by

$$W = \frac{\left(\sum_{i=1}^{n} a_i x_i\right)^2}{\sum_{i=1}^{n} (x_i - \bar{x})^2} \tag{1}$$

Jing *et al.* [7] have studied the breakdown characteristic of ester oil and have indicated that the breakdown voltage follows a normal distribution and the deviations at the lower and upper percentiles are high. It can be seen from Table 3 that the test accepts the null hypothesis of normal distribution. Further, in order to check for the extreme value distribution, the *K-S* test was carried out which indicated a lower *p*-value. Dang *et al.* [26] has confirmed that the breakdown voltage of natural ester oil follows normal distribution. Fig. 9 shows the probability plot of breakdown voltage on thermally aged ester oil under AC and DC voltages. More scatter in the data is being observed in negative DC voltage and it was higher for virgin ester oil compared to aged oil. The skewness of the observed breakdown value was positive and the kurtosis was negative for both virgin and thermally aged ester oil (Table 4) which indicates the right shift in the data spread from the mean value and the distribution is platykurtic [26].

3.3 UV absorption spectroscopic studies

Fig. 10 shows the UV absorption spectra of thermally aged ester oil. A progressive bathochromic shift is observed as the ester oil undergoes thermal aging. This observation essentially goes in line with the darkening of colour as observed visually. As Fig. 10 shows, the absorbance values saturate at ~5, and the approach to saturation occurs progressively at longer wavelengths as aging progresses. For such multichromophoric samples tending to saturation at lower wavelengths, Divya and Mishra [27] had introduced a 'derived absorbance' parameter as shown in (2) that corresponds to absorbance values at which inner filter effects caused loss of observed fluorescence.

$$F_{l/2,\lambda} = K \cdot A_\lambda \cdot 10^{-A_\lambda/2} \tag{2}$$

where $F_{l/2}$ is the intensity of fluorescence, A_λ is absorbance and *K* is constant factor.

The wavelengths corresponding to the maxima of such plots can be used as a quantitative parameter for estimating the progressive colouration as shown in Table 5. Derived absorbance plots as shown in Fig. 10 gives a clear idea regarding the excitation maximum as well as the shift of absorbance maximum with varying in aging period. Saha *et al.* [28] carried out UV analysis with thermally aged mineral oil and indicated that the absorbance of oil builds up monotonically with aging time at a much higher rate in the air than in nitrogen. The absorption spectra observed under high-aging temperature had a peak absorbance at a wavelength of 275 nm, and small spikes were also observed at 315 nm. These two absorption wavelengths detected were found to be due to copper ions (NIST database), which has resulted due to the erosion of copper sheets impregnated along with pressboard. The formation of acids and other compounds formed during the thermal aging process would have caused corrosion to copper material. Thus the presence of copper ions in oil is one of the indicators of degradation of oil.

Table 3 Hypothesis test of conformity to normal distribution under different voltage profiles

Sample	AC voltage		+ DC voltage		−DC voltage	
	Statistic (*W*)	*p*-value	Statistic (*W*)	*p*-value	Statistic (*W*)	*p*-value
Virgin	0.9408	0.2489	0.9781	0.7883	0.9431	0.2745
90°C	0.9458	0.3079	0.9149	0.0789	0.9355	0.1973
140°C	0.9417	0.2579	0.9705	0.7652	0.9252	0.1248
160°C	0.9281	0.1421	0.9311	0.1623	0.9301	0.1550

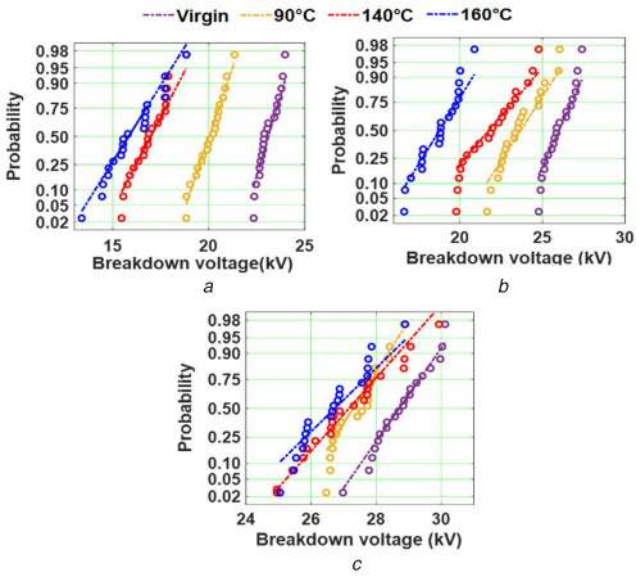

Fig. 9 *Normal probability of breakdown voltage on thermally aged ester oil*
(a) AC voltage, ***(b)*** + DC voltage, ***(c)*** −DC voltage

Table 4 Skewness and Kurtosis of thermally aged ester oil for breakdown voltage under AC and DC voltage

Sample	AC voltage		+ DC voltage		−DC voltage	
	Skewness	Kurtosis	Skewness	Kurtosis	Skewness	Kurtosis
Virgin	0.3900	−1.1329	0.1484	−1.2946	0.0436	−0.4406
90°C	0.2175	−0.6836	0.4851	−0.6731	0.2065	−0.9792
140°C	0.0890	−0.5566	0.1911	−1.1407	0.2583	−0.4838
160°C	0.1909	−0.3907	0.2567	−0.8576	0.3921	−0.5276

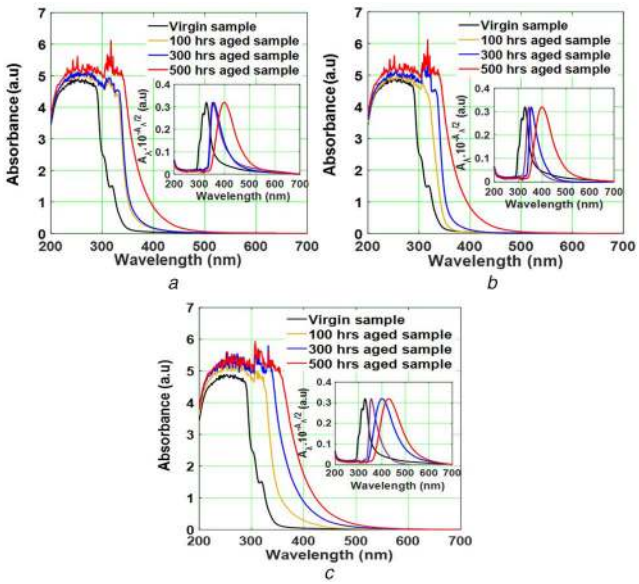

Fig. 10 *Variation in UV absorption spectrum of ester oil aged at different temperatures*
(a) 90°C, ***(b)*** 140°C, ***(c)*** 160°C

Table 5 Parametric variations on spectral characteristics of oil under different temperatures

Sample	Wavelength corresponding to maximum derived absorption spectra (λ_{der}^{max}) nm		
Virgin	330		
	Aging temperature, °C		
Aging time	90	140	160
100 h aged	354	342	356
300 h aged	359	356	402
500 h aged	400	400	432

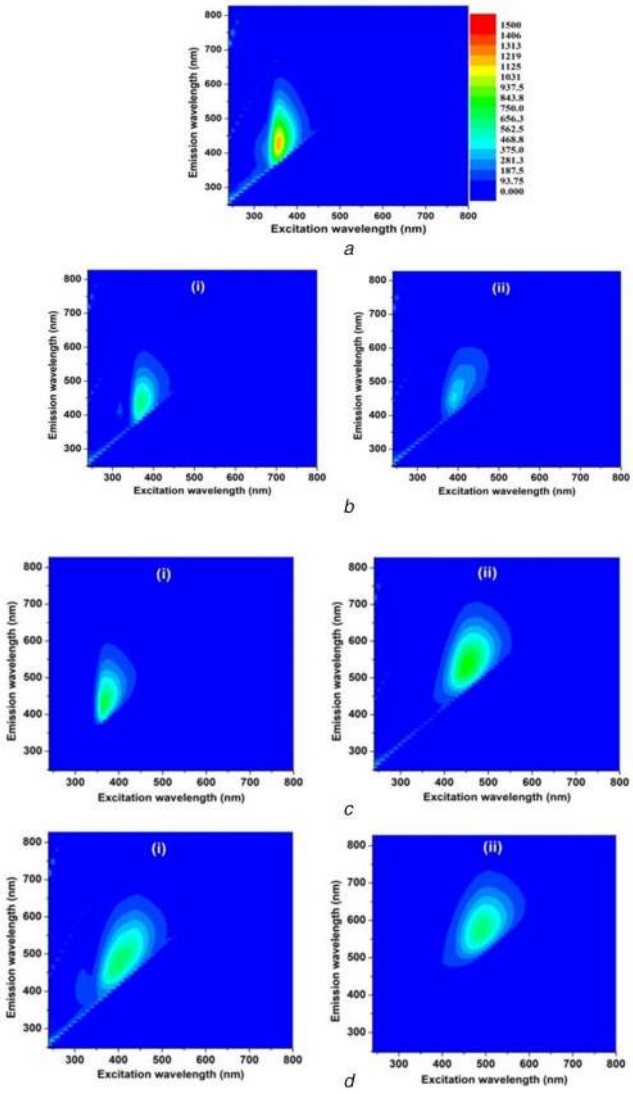

Fig. 11 *EEM spectra of*
(a) Virgin ester oil, ***(b)*** Ester oil aged at 90°C for aging duration of (i) 100 h and (ii) 500 h, ***(c)*** Ester oil aged at 140°C for aging duration of (i) 100 h and (ii) 500 h, ***(d)*** Ester oil aged at 160°C for aging duration of (i) 100 h and (ii) 500 h

3.4 Steady-state analysis of fluorescence with excitation–emission matrix (EEM) for thermally aged ester oil

Fig. 11 shows EEM spectra of virgin oil and thermally aged ester oil. The excitation maximum of oil lies in the range of 300–450 nm for both virgin oil and oil aged at a lower temperature for 100 h. On the contrary, there was a prominent Stokes shift observed when the sample was aged at a higher temperature for long duration. From the EEM spectra and the derived absorbance plot, it is clear that there is a close correspondence with the aging and redshift of excitation maximum.

From derived absorbance plot (Fig. 10) the λ_{max} of virgin sample is 330 nm and it is nearly same as the excitation maximum of the virgin sample in EEM contour map (Fig. 11). Similar behaviour can be clearly observed from derived absorbance plot and EEM spectra of aged samples. This close correspondence is summarised well in Tables 5 and 6.

The change in the composition of the oil, as observed from GC/MS analysis (Table 7), could also be a reason for the the concentration-dependent red shift. The emission maxima of virgin oil lying at 425 nm were only slight shifted by about 10 nm when the aging was carried out at lower temperatures (90°C). On the other hand, there was a substantial change in its shift by nearly 50 nm when the the aging temperature was higher, i.e. 140, 160°C. Fig. 12 shows the increase in λ_{der}^{max} value with aging it closely corresponds to the shift in the λ excitation maximum of EEM contour maxima. This work shows that an understanding of the characteristic changes in the EEM spectra of the insulation oil and its correlation with the insulation-relevant properties of the oil can be a valuable input to assess the quality of the oil in real-time, to use as an insulant.

Table 6 Parametric variations on the EEM spectra of oil under different temperatures

Sample	Excitation maxima, nm			Emission maxima, nm		
Virgin	350			425		
	Aging temperature, °C					
Aging time	90	140	160	90	140	160
100 h-aged sample	360	370	400	435	475	476
500 h-aged sample	390	440	480	450	535	570

Table 7 Composition of thermally aged ester oil based on GC-MS data

Organic groups/compounds	Selectivity, %			
	Virgin sample	100 h aged	300 h aged	500 h aged
carboxylic acids and acid anhydrides	4.20 (88–90%)	16.60 (88–90%)	42.10 (88–90%)	47.1 (88–90%)
9,12-octa decadienoic acid ($C_{18}H_{32}O_2$)	4.20 (92%)	14.20 (92%)	19.00 (92%)	22.4 (92%)
decanoic acid,3-methyl ($C_{11}H_{22}O_2$)	0.0	0.0	19.00 (87%)	21.0 (87%)
carbonyl compounds	2.80 (85–90%)	4.30 (85–90%)	3.80 (85–90%)	11.2 (85–90%)
4-heptanone 2,2,3,3,5,5,6,6-octamethyl ($C_{15}H_{30}O$)	0.0	0.0	0.0	4.30 (86%)
4-heptanone,5,5-diethyl-2,2,3,3-tetramethyl ($C_{15}H_{30}O$)	0.0	3.60 (89%)	3.20 (89%)	3.30 (89%)
antioxidants(α-tocopherol-β-mannoside and γ-tocopherol) ($C_{28}H_{48}O_2$)	3.20 (88–90%)	1.30 (88–90%)	2.82 (88–90%)	0.0

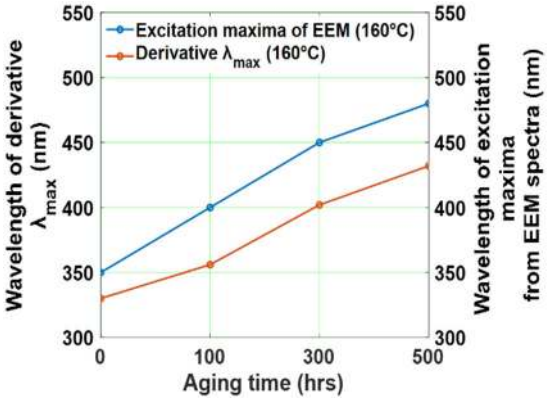

Fig. 12 *Comparison of EEM excitation maximum and λ_{der}^{max} of ester oil at 160°C aging*

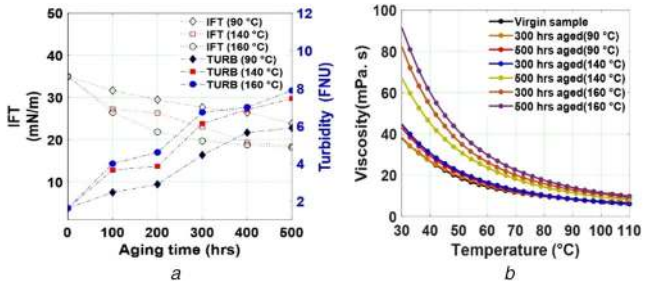

Fig. 13 *Chemical analysis of ester oil aged at different temperatures*
(a) IFT and turbidity, ***(b)*** Viscosity

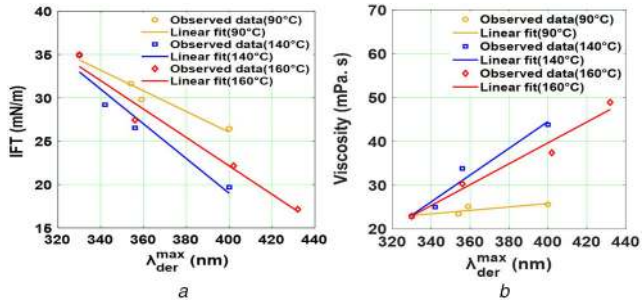

Fig. 14 *Correlation between the maximum wavelength of derivative absorption spectra with*
(a) IFT, ***(b)*** Viscosity

3.5 Chemical properties of thermally aged ester oil

The variations in the IFT, turbidity and viscosity of the thermally aged ester oil are shown in Fig. 13. It was observed that the turbidity of the oil increases with aging due to contamination of solid particles in the suspension. Oil decolouration was also observed with degradation due to insoluble colloidal suspensions produced by oil and the pressboard. A drastic reduction in IFT was observed due to thermal aging. The attraction between the water molecules at the interface was influenced by the presence of polar molecules in suspension with the oil that has caused a decrease in its IFT. Moreover, the red shift in the absorption characteristics of aged oil, possibly due to polar solvents, was confirmed by the variation in its IFT value for thermally degraded oil sample. It is found that viscosity of oil varies with the aging temperature. At low aging temperatures, no significant variation in viscosity was observed, while characteristic variations are observed at higher temperatures.

The correlation between λ^{max} of derived absorption spectra (λ_{der}^{max}) and chemical characteristics of thermally aged ester oil is shown in Fig. 14. Baka *et al.* [29] estimated the IFT value based on the absorption peak of the thermally aged transformer oil. In the present study, a strong correlation of IFT and viscosity with derived absorption maxima is observed. A direct linear relation exists between viscosity and λ_{der}^{max}, whereas inverse linear trend was observed between IFT and λ_{der}^{max}. The observed correlation factor was high, as the goodness of fit lies in the range of 0.9743–0.9985. The results of the study clearly indicate that λ_{der}^{max} has a direct correlation to the chemical property of thermally aged oil and is predominant when thermal aging is carried out at higher temperatures.

3.6 Organic composition of thermally aged ester oil

The virgin and thermally aged ester oils were analysed for their composition using GC/MS. The GC/MS analysis was carried out only for the samples aged at high temperature (160°C) due to significant variation in the organic composition as compared to that aged at a low temperature of 90°C. The relative composition or percent selectivity of major organic functional groups in the virgin and aged oils are shown in Table 7. The percentage match of the individual organic compound and that of the functional group with NIST MS database is indicated in parenthesis. It is evident that the selectivity's of oxygenated species like carboxylic acids, and carbonyl compounds are increasing with the increase in the aging time. This is a clear indication of thermal oxidation of the ester oil. Carboxylic acids and ketones are formed via elementary autoxidation pathways involving free radical reactions such as

alkoxy radical β-scission, alkyl radical β-scission, hydrogen transfer and disproportionation [30]. Bandara *et al.* [31] have indicated that at high-temperature moisture migrates from pressboard to oil and enhances the hydrolytic degradation of natural ester.

4 Conclusion

The important conclusions accrued based on the present study are

- It is observed that the aging temperature and duration have high impact on PDIV and breakdown voltage of ester oil. The PDIV is high under negative DC voltage followed with positive and AC voltage. The impact of high-frequency AC voltage on PD activity was very minimal. Similarly under harmonic AC voltage, only a marginal reduction was inferred at higher THD's. The Weibull distribution studies with PDIV measurement indicate a reduction in the scale parameter (α) for the thermally aged oil, at different temperatures, under different voltage profiles.
- PRPD analysis under harmonic AC voltages with THD's were studied and found that the discharges always occur when the rate of change of voltage is high. Based on PRPD analysis, the number of discharges formed due to PD activity with virgin and thermally aged ester oil, are same.
- Reduction in breakdown voltage was observed with the thermally aged ester oil, under AC, DC and standard lightning impulse voltages. The negative lightning impulse showed a higher breakdown voltage followed by positive lightning and DC voltages. The breakdown voltage of thermally aged ester oil follows a normal distribution and platykurtic, which was confirmed through hypothesis test.
- IFT and turbidity followed an inverse relationship with thermally aged ester oil and have a close correlation with $\lambda_{\text{der}}^{\max}$. The GC/MS organic composition analysis showed the formation of more carboxylic acids and ketones with aging duration. This is a suggestive indication of an oxidative cleavage pathway of the ester oil during thermal aging process.
- EEM analysis of ester oil aged at 140 and 160°C showed a uniform shift of emission of about 50 nm while at lower temperature like 90°C the shift was only 10 nm. An increase in the $\lambda_{\text{der}}^{\max}$ and the presence of copper ions were identified through UV absorption spectra of thermally aged ester oil.
- For aged oil samples with absorption saturation, a derived absorbance plot seems to correlate well with the excitation maximum of the fluorescence signal. Moreover, the viscosity dependence on the $\lambda_{\text{der}}^{\max}$ also showed a direct relationship with thermally aged natural ester oil.

5 References

[1] N'cho, J.S., Fofana, I., Hadjadj, Y., *et al.*: 'Review of physicochemical-based diagnostic techniques for assessing insulation condition in aged transformers', *Energies*, 2016, **9**, (5), p. 367

[2] Saha, T.K., Purkait, P.: '*Transformer ageing*' (John Wiley & Sons Singapore Pte. Ltd, Singapore, 2017)

[3] Singha, S., Asano, R., Frimpong, G., *et al.*: 'Comparative aging characteristics between a high oleic natural ester dielectric liquid and mineral oil', *IEEE Trans. Dielectr. Electr. Insul.*, 2014, **21**, (1), pp. 149–158

[4] Mehta, D.M., Kundu, P., Chowdhury, A., *et al.*: 'A review on critical evaluation of natural ester vis-a-vis mineral oil insulating liquid for use in transformers: part 1', *IEEE Trans. Dielectr. Electr. Insul.*, 2016, **23**, (2), pp. 873–880

[5] Fernandez, F.O., Ortiz, A., Delgado, F., *et al.*: 'Transformer health indices calculation considering hot-spot temperature and load index', *IEEE Electr. Insul. Mag.*, 2017, **33**, (2), pp. 35–43

[6] Loiselle, L., Fofana, I., Sabau, J., *et al.*: 'Comparative studies of the stability of various fluids under electrical discharge and thermal stresses', *IEEE Trans. Dielectr. Electr. Insul.*, 2015, **22**, (5), pp. 2491–2499

[7] Jing, Y., Timoshkin, I.V., Wilson, M.P., *et al.*: 'Dielectric properties of natural ester, synthetic ester midel 7131 and mineral oil diala D', *IEEE Trans. Dielectr. Electr. Insul.*, 2014, **21**, (2), pp. 644–652

[8] Sonerud, B., Bengtsson, T., Blennow, J., *et al.*: 'Dielectric heating in insulating materials subjected to voltage waveforms with high harmonic content', *IEEE Trans. Dielectr. Electr. Insul.*, 2009, **16**, (4), pp. 926–933

[9] Stone, G.C.: 'Partial discharge diagnostics and electrical equipment insulation condition assessment', *IEEE Trans. Dielectr. Electr. Insul.*, 2005, **12**, (5), pp. 891–904

[10] Judd, M.D., Cleary, G.P., Bennoch, C.J.J.: 'Applying UHF partial discharge detection to power transformers', *IEEE Power Eng. Rev*, 2002, **22**, (8), pp. 57–59

[11] Huang, Y.M., Liu, Q., Wang, Z.D.: 'Effects of temperature on partial discharge and breakdown characteristics of an ester liquid under AC stress'. IEEE Int. Conf. on High Voltage Engineering and Application (ICHVE), Athens, Greece, 2018, pp. 1–4

[12] Florkowski, M., Florkowska, B., Furgal, J., *et al.*: 'Impact of high voltage harmonics on interpretation of partial discharge patterns', *IEEE Trans. Dielectr. Electr. Insul.*, 2013, **20**, (6), pp. 2009–2016

[13] Rozga, P.: 'Streamer propagation and breakdown in a very small point-insulating plate gap in mineral oil and ester liquids at positive lightning impulse voltage', *Energies*, 2016, **9**, (6), p. 467

[14] Marin-Serrano, A., Balderas-Lopez, J.A., Calva, P., *et al.*: 'Thermo-optical properties as complementary parameters for damage assessment of mineral oils aged under controlled conditions used in power transformers', *Thermochim. Acta*, 2019, **676**, pp. 33–38

[15] Bessant, C., Ritchie, L., Saini, S., *et al.*: 'Chemometric evaluation of synchronous scan fluorescence spectroscopy for the determination of regulatory conformance and usage history of insulation oils', *Appl. Spectrosc*, 2001, **55**, (7), pp. 840–846

[16] Sikorska, E., Romaniuk, A., Khmelinskii, I.V., *et al.*: 'Characterization of edible oils using total luminescence spectroscopy', *J. Fluoresc.*, 2004, **14**, (1), pp. 25–35

[17] Judd, M.D., Farish, O.: 'A pulsed GTEM system for UHF sensor calibration', *IEEE Trans. Instrum. Meas*, 1998, **47**, (4), pp. 875–880

[18] IEC TS 62332-2: 'Electrical insulation systems (EIS) – thermal evaluation of combined liquid and solid components – part 2: simplified test', 2014

[19] Lesaint, O., Top, T.V.: 'Streamer initiation in mineral oil. Part I: electrode surface effect under impulse voltage', *IEEE Trans. Dielectr. Electr. Insul.*, 2002, **9**, (1), pp. 84–91

[20] Azcarraga, C.G., Cavallini, A., Piovan, U.: 'A comparison of the voltage withstand properties of ester and mineral oils', *IEEE Electr. Insul. Mag.*, 2014, **30**, (5), pp. 6–14

[21] Xiang, J., Liu, Q., Wang, Z.D.: 'Inception and breakdown voltages of insulating liquids under DC stress'. IEEE Int. Conf. on High Voltage Engineering and Application (ICHVE), Chengdu, China, 2016, pp. 1–4

[22] IEC 62539: 'Guide for the statistical analysis of electrical insulation breakdown data', 2007

[23] Lawless, J.F.: '*Statistical models and methods for lifetime data*' (John Wiley & Sons, USA, 2011)

[24] Dang, V.H., Beroual, A., Perrier, C.: 'Investigations on streamers phenomena in mineral, synthetic and natural ester oils under lightning impulse voltage', *IEEE Trans. Dielectr. Electr. Insul.*, 2012, **19**, (5), pp. 1521–1527

[25] Li, J., Chen, X., Xu, Y., *et al.*: 'Effect of acid value on breakdown performance of vegetable insulating oil under lighting impulse'. Proc. IEEE Int. Conf. on Dielectr Liquids (ICDL), Manchester, UK, 2017, pp. 1–4

[26] Dang, V.H., Beroual, A., Perrier, C.: 'Comparative study of statistical breakdown in mineral, synthetic and natural ester oils under AC voltage', *IEEE Trans. Dielectr. Electr. Insul.*, 2012, **19**, (5), pp. 1508–1513

[27] Divya, O., Mishra, A.K.: 'Understanding the concept of concentration-dependent red-shift in synchronous fluorescence spectra: prediction of λ SFSmax and optimization of $\Delta\lambda$ for synchronous fluorescence scan', *Anal. Chim. Acta*, 2008, **630**, (1), pp. 47–56

[28] Saha, T.K., Darveniza, M., Yao, Z.T.: 'Investigating the effects of oxidation and thermal degradation on electrical and chemical properties of power transformers insulation', *IEEE Trans. Power Deliv.*, 1999, **14**, (4), pp. 1359–1367

[29] Baka, N.A., Abu-Siada, A., Islam, S.: 'A new technique to measure interfacial tension of transformer oil using UV-Vis spectroscopy', *IEEE Trans. Dielectr. Electr. Insul.*, 2015, **22**, (2), pp. 1275–1282

[30] Pfaendtner, J., Broadbelt, L.J.: 'Mechanistic modeling of lubricant degradation. 1. Structure − reactivity relationships for free-radical oxidation', *Ind. Eng. Chem. Res.*, 2018, **47**, (9), pp. 2886–2896

[31] Bandara, K., Ekanayake, C., Saha, T.K., *et al.*: 'Understanding the ageing aspects of natural ester based insulation liquid in power transformer', *IEEE Trans. Dielectr. Electr. Insul.*, 2016, **23**, (1), pp. 246–257